Int. J. Solids Structures Vol. 25, No. 1, pp. 75–93, 1989
Printed in Great Britain.

0020–7683/89 $3.00 + .00

ON THE SIGNIFICANCE OF THE LOGARITHMIC TERM IN THE FREE EDGE STRESS SINGULARITY OF COMPOSITE LAMINATES

H. K. STOLARSKI and M. Y. M. CHIANG†
Department of Civil Engineering, Mechanics and Metallurgy,
University of Illinois at Chicago, P.O. Box 4348, Chicago, IL 60680, U.S.A.

(*Received* 6 *August* 1987; *in revised form* 16 *August* 1988)

Abstract—Composite laminates under axial stretching are analyzed by means of the enriched finite elements. The r^δ singularity and $\log r$ singularity are included to describe the edge effects. It is concluded that, in general, they are both necessary if reliable information about the strength of those singularities is to be obtained.

1. INTRODUCTION

Recent investigations (Ting and Chou, 1981; Zwiers *et al.*, 1982), have shown that, with the exception of the $(\theta/-\theta)$ composite and a special θ/θ' family of composites, the logarithmic stress singularity at the free edge of composite laminates is present irrespective of the conditions on the boundary remote from the singular point. This is in contrast with the more common r^δ $(-1 < \delta < 0)$ stress singularity (Wang and Choi, 1982a, b; Zwiers *et al.*, 1982), which may exist at the free edge of any laminate, but the actual presence of which cannot be ascertained until the complete boundary value problem is solved.

Although the presence of the logarithmic singularity may, of course, be sufficient to cause delamination at the free edge of the composite, the role of the possible r^δ singularity should not be ignored. The r^δ singularity is much stronger than the logarithmic singularity and, if present, can be primarily responsible for the onset of delamination. It is therefore worthwhile to examine relative importance of the two singularities, their interaction and their influence on the stress distribution. This task is however beyond the reach of the analytic approach. The finite element technique incorporating analytical results of the asymptotic analysis is used in this paper to gain some insight into the problem.

It has been found in the past that as far as the stress distribution in problems involving singularities is concerned even standard techniques, such as properly processed usual (non-singular) finite elements, have high predicting capabilities (Rybicki, 1971; Herakovich, 1976; Herakovich *et al.*, 1976; Wang and Crossman, 1977) (as do other methods which can be found in Pipes and Pagano (1970), Gallagher (1971), Pagano (1974, 1978), Tang (1975), Tang and Levy (1975), Altus *et al.* (1980), Spilker and Chou (1980), Ting and Chou (1981), Wang and Dickson (1978), Wang and Choi (1982a, b) and Wang and Yuan (1983)). Only in the immediate vicinity of the singular point, the solution obtained in such a standard way is not accurate and its convergence is generally very slow (Tong and Pian, 1973). The stresses around and at the singular point obtained by means of standard finite element techniques are finite, although the stress gradients are usually high indicating the presence of a singularity. However, once analytical methods, such as asymptotic techniques, establish the possible existence and order of the singularity, the numerical techniques can incorporate the analytical results to provide complete and accurate information characterizing the solution. In addition to the stress distribution away from the singular point, they can then give accurate values of the strength of the existing singularities, i.e. the stress intensity factors. In fact, the stress intensity factors may be even more important than the stress distribution away from the singular point since, in most cases, intensity of the stresses at the singular point may be directly linked to the initiation of delamination. Thus, the calculation of the stress intensity factors is stressed herein.

† Present address: Polymers Division, National Bureau of Standards, Gaithersburg, MD 20899, U.S.A.

The point of view expressed above guided researchers in many different ways and, consequently, various finite element approaches providing complete solutions to problems involving singularities have been developed by Hartranft and Sih (1969), Byskov (1970), Pian *et al.* (1971), Tong *et al.* (1973), Atluri *et al.* (1975), Lin and Mar (1976) and Bartholomew (1978). In this paper the enriched finite element technique has been selected. These elements, known also as global/local finite elements (Morley, 1970; Mote, 1971), have been successfully used in the analysis of singularities (Benzley, 1974; Chen, 1985). The major idea consists of introducing the analytic, singular part of the solution, defined over the entire domain of the problem, and supplementing it with the regular part, constructed by standard (nonsingular) finite elements. Arguments behind this particular selection are given further in the paper.

In the presentation of the material, full development of the expressions defining the singular part of the solution (and needed herein) will not be provided, for details the reader is referred to Zwiers *et al.* (1982). However, for the paper to be self-contained, the major steps leading to such expressions are outlined in the Appendix and the final results are quoted in Section 2. The enriched finite element technique is briefly described in Section 3, and the numerical results are presented in Section 4. Conclusions form the last section, Section 5, of the paper.

2. SPECIFICATION OF THE PROBLEM AND NEEDED ANALYTICAL RESULTS

This paper is concerned with the analysis of the laminated composite specimen shown in Fig. 1. The composite is stretched along its longest dimension, parallel to the x^1-axis. It

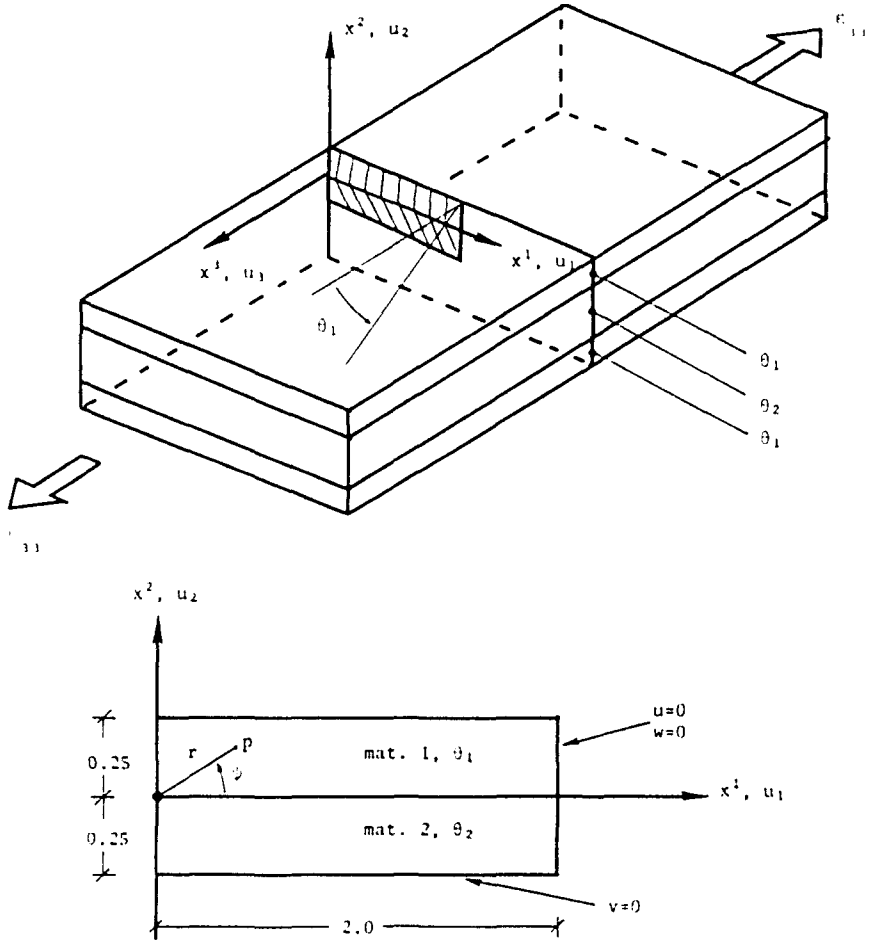

Fig. 1. Specification of the problem.

is assumed that each lamina is an orthotropic material with the principal directions $\bar{x}^1$, $\bar{x}^2$, $\bar{x}^3$ where $\bar{x}^2 = x^2$ (Fig. 1). The remaining two principal axes lie in the (x^1, x^3) plane; the third principal direction is parallel to the fibers and makes an angle θ with the x^3-axis. As opposed to most works dealing with the problem (in fact the authors know of only two exceptions: Zwiers *et al.* (1982) and Davet and Destuynder (1986)) the orientation θ of the material in each layer is arbitrary (i.e. $\theta_1 \neq -\theta_2$).

For the purpose of calculation and comparison it is further assumed that all layers are formed of the same material (high modulus graphite/epoxy) the constants of which, related to the principal directions, are

$$\begin{aligned} E_1 &= E_2 = 2.1 \times 10^6 \text{ psi} \\ E_3 &= 20.0 \times 10^6 \text{ psi} \\ G_{12} &= G_{23} = G_{31} = 0.85 \times 10^6 \text{ psi} \\ \nu_{21} &= \nu_{31} = \nu_{32} = 0.21. \end{aligned} \tag{1}$$

This specification is not essential and assuming different materials in different layers incurs no additional difficulty as long as the position of the principal directions of orthotropy remains as described above. The analysis will be related to the central section of the specimen, remote from the point of application of the load, where the three displacement components u_i, $i = 1, 2, 3$ can be assumed to depend only on x^1 and x^2 (Fig. 1). This condition is combined with the assumption $\varepsilon_{33} = \text{const.}$, which characterizes the amount of stretching (Zwiers *et al.*, 1982). Since the problem is linear we have assumed $\varepsilon_{33} = 1.0$.

An asymptotic analysis based on the above assumptions revealed that, in general, two different types of singularity may occur at the free edge of the interface if $\theta_1 \neq -\theta_2$ (Zwiers *et al.*, 1982). As a result of this analysis one of those singularities, of the type r^δ ($\delta < 0$), is defined within a multiplicative constant, representing its strength. The constant itself remains, however, unknown until the entire boundary value problem is solved. The second singularity, of the log r type, emerges fully determined (i.e. including the multiplier).

Displacement fields associated with the above singularities have been derived in Zwiers *et al.* (1982). For the convenience of the reader the method of derivation is sketched in the Appendix. It is found that the log r singularity is associated with the following fully determined displacement field:

$$\hat{u}_i^1 = \sum_{L=1}^{3} \{G_L \operatorname{Re}[v_{i,L} Z_L (\ln Z_L - 1)] + H_L \operatorname{Im}[v_{i,L} (\ln Z_L - 1)]\} \tag{2a}$$

while the r^δ singularity with the field

$$\hat{u}_i^2 = \sum_{L=1}^{3} \{A_L \operatorname{Re}(v_{i,L} Z_L^{1+\delta}) + B_L \operatorname{Im}(v_{i,L} Z_L^{1+\delta})\}/(1+\delta) \tag{2b}$$

in which the unknown constant mentioned earlier is not included. All of the quantities appearing in eqns (2a) and (2b) are determined as a result of the analysis presented in Zwiers *et al.* (1982); Z_L is a specified linear complex function of x^1 and x^2 (Fig. 1), $v_{i,L}$, $L = 1, 2, 3$ are determined complex numbers, δ as well as A_L, B_L, G_L, H_L, $L = 1, 2, 3$ are determined real numbers, which depend on stacking sequence and material properties of the composite. Consequently eqns (2a) and (2b) should be viewed as known, real functions of x^1 and x^2.

In fact the functions given in eqns (2a) and (2b) are different within each layer since $v_{i,L}$ and Z_L as well as A_L, B_L, G_L and H_L differ from layer to layer. Continuity of these functions and of the related stresses at the interface is however guaranteed; thus eqns (2a) and (2b) evaluated properly in each layer represent actually one continuous function, defined over the entire domain of the problem.

The functions given in eqns (2a) and (2b) will be used within the finite element scheme described in the next section.

3. BASIC FEATURES OF THE FINITE ELEMENT TECHNIQUE USED

Consider a problem involving singularities and suppose that orders of all those singularities have been identified. Let the displacement field associated with the singularity α be $\hat{u}_i^{\alpha}(x^j)$ where x^j represents a (Cartesian) coordinate system. In general we may have Λ singularities, so $\alpha = 1, 2, \ldots, \Lambda$, which are located in the same or different physical point of the domain. In the particular case considered in this paper we have $\Lambda = 1$ in case of the $(\theta_i - \theta)$ composite and $\Lambda = 2$ for the general (θ_1/θ_2) composites. In the latter case both singularities occur at the same point located at the free edge of the interface.

With the data described above known we will follow the procedure described by Benzley (1974) (see also in Morley (1970), Mote (1971) and Chen (1985)). Thus, the total displacement field is represented as follows:

$$u_i(x^k) = \sum_{\alpha=1}^{\Lambda} c_\alpha \hat{u}_i^{\alpha}(x^k) + \hat{u}_i^{r}(x^k) \tag{3}$$

where $\hat{u}^r$ represents the regular part of the solution (having no singularity) and c_α is either a known, if the singularity α is fully determined, or is an unknown displacement parameter, if the singularity α is determined within a multiplicative constant (the latter is a more common situation). The regular part of eqn (3) is approximated by a standard finite element technique

$$\hat{u}_i^{r}(x^k) = \sum_{l=1}^{n} \phi_{il}(x^k)\hat{d}_{il} \tag{4}$$

with ϕ_{il} being the approximating functions and $\hat{d}_{il}$ related displacement parameters; n is the total number of nodal points.

Since the singular part of eqn (3) is defined over the entire domain of the problem, it is clear that $\hat{d}_{il}$ constitute only a part of nodal displacements; the remaining part comes from $\hat{u}_i^{\alpha}$. This is inconvenient when the kinematic boundary conditions are to be imposed. To avoid this inconvenience the interpolant of $\hat{u}_i^{\alpha}$ obtained by means of the approximating functions ϕ_{il} has been subtracted from the singular part of the approximation and added to the regular part of it. Thus

$$\begin{aligned} u_i &= \sum_{\alpha=1}^{\Lambda} c_\alpha \hat{u}_i^{\alpha} + \hat{u}_i^{r} = \sum_{\alpha=1}^{\Lambda} c_\alpha \left(\hat{u}_i^{\alpha} - \sum_{l=1}^{n} \phi_{il}\hat{u}_{il}^{\alpha} \right) + \sum_{l=1}^{n} \phi_{il} \left(\hat{d}_{il} + \sum_{\alpha=1}^{\Lambda} c_\alpha \hat{u}_{il}^{\alpha} \right) \\ &= \sum_{\alpha=1}^{\Lambda} c_\alpha u_i^{\alpha} + \sum_{l=1}^{n} \phi_{il} d_{il} \end{aligned} \tag{5}$$

where

$$u_i^{\alpha} = \hat{u}_i^{\alpha} - \sum_{l=1}^{n} \phi_{il}\hat{u}_{il}^{\alpha} \tag{6a}$$

$$d_{il} = \hat{d}_{il} + \sum_{\alpha=1}^{\Lambda} c_\alpha \hat{u}_{il}^{\alpha}. \tag{6b}$$

Now u_i^{α} vanishes at the nodal points and d_{il} represent total nodal displacements. Since for any given $\hat{u}_i^{\alpha}$ evaluation of u_i^{α} as defined in eqn (6a) is straightforward, use of eqn (5) rather than eqns (3) and (4) is simple and removes the inconvenience associated with displacement boundary conditions (Benzley, 1974).

With the above explanation the rest of the formulation follows all of the steps of the usual displacement formulation. To be concise we will delineate them using matrix notation typical for this formulation. Thus the displacement field of eqn (5) is written on the element

level in the following form:

$$\mathbf{u} = [\mathbf{N}^r, \mathbf{N}^s] \begin{Bmatrix} \mathbf{d}^r \\ \mathbf{d}^s \end{Bmatrix} = \mathbf{N}\mathbf{d} \tag{7}$$

where

$$\mathbf{u} = [u_1, u_2, u_3]^T \tag{8a}$$

$$\mathbf{N}^r = [\mathbf{N}_1, \mathbf{N}_2, \mathbf{N}_3, \ldots, \mathbf{N}_n] \tag{8b}$$

$$\mathbf{N}_I = \begin{bmatrix} \phi_{1I} & 0 & 0 \\ 0 & \phi_{2I} & 0 \\ 0 & 0 & \phi_{3I} \end{bmatrix}, \quad \phi_{iI} = \phi_{iI}(x^1, x^2) \tag{8c}$$

$$\mathbf{N}^s = \begin{bmatrix} u_1^1 & u_1^2 & \ldots & u_1^\Lambda \\ u_2^1 & u_2^2 & \ldots & u_2^\Lambda \\ u_3^1 & u_3^2 & \ldots & u_3^\Lambda \end{bmatrix} \tag{8d}$$

$$\mathbf{d}^r = [\mathbf{d}_1^T, \mathbf{d}_2^T, \ldots, \mathbf{d}_n^T]^T, \quad \mathbf{d}_I^T = [d_{1I}, d_{2I}, d_{3I}] \tag{8e}$$

$$\mathbf{d}^s = [c_1, c_2, \ldots, c_\Lambda]^T. \tag{8f}$$

If the operator defining $\bar{\varepsilon}$ of eqn (A4) in the Appendix is denoted by $\mathbf{L}$ one gets

$$\bar{\varepsilon} = \mathbf{L}\mathbf{u} = \mathbf{L}\mathbf{N}\mathbf{d} = \mathbf{B}\mathbf{d} = [\mathbf{B}^r, \mathbf{B}^s] \begin{Bmatrix} \mathbf{d}^r \\ \mathbf{d}^s \end{Bmatrix} \tag{9}$$

where

$$\mathbf{B}^r = \mathbf{L}\mathbf{N}^r \tag{10a}$$

$$\mathbf{B}^s = \mathbf{L}\mathbf{N}^s. \tag{10b}$$

Equation (9) does not include ε_{33} which reflects the fact that the problem is independent of x^3 and implies that ε_{33} = constant (we assume $\varepsilon_{33} = 1$).

To obtain the finite element equations the principle of virtual work is used. For a two-dimensional domain in the absence of the external forces the principle has the following form:

$$\int_A \delta\boldsymbol{\varepsilon}^T \boldsymbol{\sigma}\, dA = 0 \tag{11}$$

where $\boldsymbol{\sigma}$ is the stress tensor and A represents the area of the domain. In view of the assumption $\varepsilon_{33} = 1$, we have $\delta\varepsilon_{33} = 0$ thus only $\bar{\varepsilon}$ undergo variation, but the stresses $\boldsymbol{\sigma}$ depend on both the five strain components included in $\bar{\varepsilon}$ of eqn (9) and $\varepsilon_{33} = 1$. Considering this fact along with eqn (9) the following expression is obtained from eqn (11):

$$\sum_e \delta\mathbf{d}^T \left[\left(\int_{A^e} \mathbf{B}^T \mathbf{C}_{11} \mathbf{B}\, dA \right) \mathbf{d} + \int_{A^e} \mathbf{B}^T \mathbf{C}_{12}\, dA \right] = 0 \tag{12}$$

where A^e is the area of element e, $\mathbf{C}_{11}$ is the 5×5 submatrix of the 6×6 constitutive matrix $\mathbf{C}$, corresponding to the five strain components included in vector $\bar{\varepsilon}$ and $\mathbf{C}_{12}$ is the 5×1 submatrix of $\mathbf{C}$ which corresponds to $\bar{\varepsilon}$ and ε_{33}. Equation (12) clearly shows that the finite

element equations

$$\mathbf{K}\mathbf{d} = -\mathbf{f} \tag{13}$$

can be obtained by assembling $\mathbf{K}$ and $\mathbf{f}$ from the following element matrices:

$$\mathbf{K}^e = \int_{A^e} \mathbf{B}^T \mathbf{C}_{11} \mathbf{B}\, dA \tag{14a}$$

$$\mathbf{f}^e = \int_{A^e} \mathbf{B}^T \mathbf{C}_{12}\, dA. \tag{14b}$$

Considering eqn (9) one can see that $\mathbf{K}^e$ and $\mathbf{f}^e$ are of the following form:

$$\mathbf{K}^e = \begin{bmatrix} \mathbf{K}^{rr} & \mathbf{K}^{rs} \\ (\mathbf{K}^{rs})^T & \mathbf{K}^{ss} \end{bmatrix} \tag{15a}$$

$$\mathbf{f}^e = \begin{Bmatrix} \mathbf{f}^r \\ \mathbf{f}^s \end{Bmatrix} \tag{15b}$$

where r corresponds to the regular and s to the singular terms. Since degrees of freedom $\mathbf{d}^s$ are common to all of the elements the usually banded character of the total stiffness matrix $\mathbf{K}$ is destroyed. However, if the parameters $\mathbf{d}^s$ are placed at the end of the global vector of degrees of freedom, eqn (13) has the following structure:

$$\begin{bmatrix} \mathbf{K}_{11} & \mathbf{K}_{12} \\ \mathbf{K}_{21} & \mathbf{K}_{22} \end{bmatrix} \begin{Bmatrix} \mathbf{d}^r \\ \mathbf{d}^s \end{Bmatrix} = \begin{Bmatrix} \mathbf{f}_1 \\ \mathbf{f}_2 \end{Bmatrix} \tag{16}$$

where $\mathbf{d}^r$ is the total vector of the "regular" degrees of freedom, $\mathbf{K}_{11}$, $\mathbf{K}_{12}$, $\mathbf{K}_{21} = \mathbf{K}_{12}^t$ and $\mathbf{K}_{22}$ are obtained as a result of assembly of $\mathbf{K}^{rr}$, $\mathbf{K}^{rs}$, $\mathbf{K}^{sr} = (\mathbf{K}^{rs})^t$ and $\mathbf{K}^{ss}$ of eqn (15a), respectively. In this case $\mathbf{K}_{11}$ is exactly the same as for regular finite elements. Thus solving first equations related to $\mathbf{d}^s$ and then those related to $\mathbf{d}^r$ we have

$$\mathbf{d}^r = \mathbf{K}_{11}^{-1}(\mathbf{f}_1 - \mathbf{K}_{12}\mathbf{d}^s) \tag{16a}$$

$$\mathbf{d}^s = (\mathbf{K}_{22} - \mathbf{K}_{21}\mathbf{K}_{11}^{-1}\mathbf{K}_{12})^{-1}(\mathbf{f}_2 - \mathbf{K}_{21}^{-1}\mathbf{K}_{11}\mathbf{f}_1) \tag{16b}$$

which takes full advantage of the bandedness of $\mathbf{K}_{11}$ and requires relatively little effort related to formulation and solution of eqn (16b). This is particularly true in our case since eqn (16b) represents a system of only two equations for c^1 and c^2, if c^2 is considered unknown (see the next section), or only one equation for c^1 if $c^2 = 1$.

At this point we would like to comment on the selection of the particular finite element approach just described. The approach has been selected based mainly on its extreme compatibility with the regular displacement versions of the finite element formulation. This clearly follows from eqns (15) and (16) in which $\mathbf{K}^{rr}$, $\mathbf{f}^r$ (and thus $\mathbf{K}_{11}$ and $\mathbf{f}_1$) could be obtained by the existing finite element codes. The additional calculations related to $\mathbf{K}^{rs}$, $\mathbf{K}^{ss}$ and $\mathbf{f}^s$ require only evaluation of $\mathbf{B}$, and corresponding integrals (see eqn (14a)). In view of the form of the singular fields given in eqns (2) and (5) (and in the Appendix) this task does not constitute any problem. Also, as explained in the preceding paragraph, the solution of the resulting equations takes full advantage of the banded character of the stiffness matrix corresponding to the regular terms of the approximation.

There were also other reasons behind the selection of the enriched finite element technique herein. One of them was the intention to test a different approach, which to the best of our knowledge, has not been used for this class of problems. This is important, considering that the hybrid stress approach (Wang and Yuan, 1983), or the eigenfunction

expansion (Wang and Choi, 1982a, b), seem to require considerably more effort. Another reason was the ease with which contributions of the singular terms to the stress field can be isolated not only in the neighborhood of the singular point but within the entire domain.

4. NUMERICAL RESULTS

The numerical results have been obtained for three different composite laminates: (45 / −45) laminate, (90 / 15) laminate and (−15 /75) laminate. Each layer, in all of these cases, had the same material properties given in eqn (1). To limit the volume of the results only those stress components which are continuous between the layers are evaluated at the interface (i.e. σ_{22}, σ_{23}, σ_{21}), they are responsible for delamination. Corresponding strength of both r^δ and $\log r$ contributions (stress intensity factors) are also evaluated and tabulated. They are defined respectively as coefficients S^δ_{ij} and S^l_{ij}, $ij = 22, 23, 21$, which appear in the following expansion of the interlaminar stresses (note that $x^1 = r$ in this case):

$$\sigma_{ij}(r) = S^\delta_{ij}(r)^\delta + S^l_{ij} \log r + (\text{regular terms}). \tag{17}$$

In view of the above equation it is clear that the total stress, along with its r^δ and $\log r$ contributions uniquely defined the regular part of the stress field. Because of that and because the emphasis is put in this paper on singularities the regular term seems to be the least important and, for clarity, has not been plotted in the following figures. An idea as to its magnitude can be obtained by comparing the total stress with both of the singular parts (and use of eqn (17)).

To formulate finite element equations the eigenvalue problem defined in eqn (A16) of the Appendix has to be solved first. The resulting eigenvalue $\delta_2 < 0$ ($\delta_1 = 0$, see Appendix) and corresponding (normalized) eigenvector $\mathbf{q}_2$ define the second singular term given in eqn (2b). In addition to that, for (90 /15) and (−15 /75) laminates, $\mathbf{q}_1$ has to be extracted from eqn (A21). Since $\mathbf{q}_1$ is uniquely determined (see Appendix and Zwiers *et al.* (1982)), in eqn (3) one should take $c_1 = 1$. However, to have some additional verification of the calculations, we let c_1 to be unknown and to be calculated just like c_2. Thus the value $c_1 \approx 1.0$ indicates that the procedure is correct.

All of the results which follow have been obtained with 9-node Lagrange elements and the mesh shown on Fig. 2. The selection of the mesh was to roughly preserve the total number of degrees of freedom comparing with the models used to obtain existing reference results in Wang and Yuan (1983).

While interpreting the plots representing the stress distribution along the interface one has to keep in mind that the first point at which stresses were evaluated, was at the distance

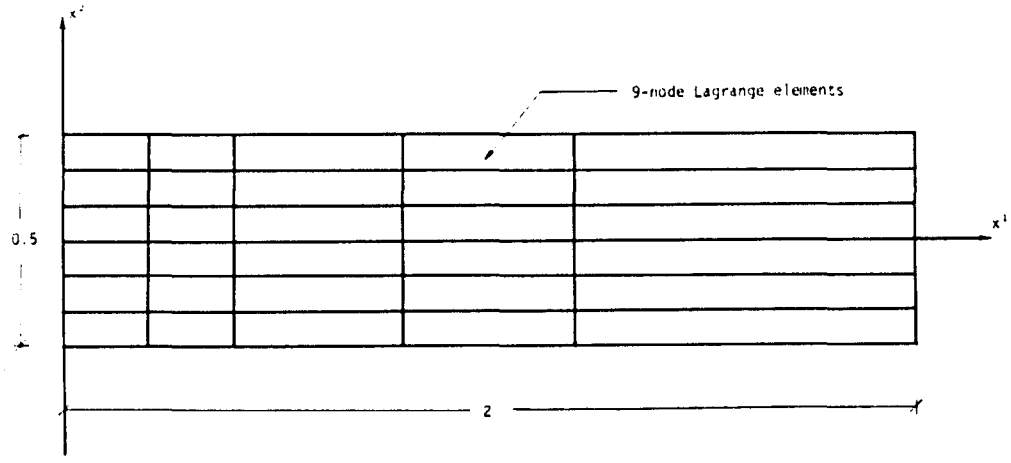

Fig. 2. Mesh used in the calculations.

Table 1. Characteristics of r^δ singularity for (45°/−45°) composite ($\delta = 0.0255757$)†

Parameter	Present results	Wang and Choi (1982a, b)
c_2	−15.248	—
S^2_{22}	−7.584	−7.535
S^2_{23}	16.551	16.443
S^1_{21}	0.000	0.000

† No log r singularity in this case (Zwiers *et al.*, 1982).

$x = 0.001003$ in. from the free edge. Thus, distribution of the stresses in the immediate vicinity of the singular point, should be qualitatively assessed based on plotted contributions of the r^δ and/or log r terms.

Furthermore, all of the stress components have been evaluated directly along the interface and resulting values for the adjacent layers have been subsequently averaged. This is different than the approach frequently used in the finite elements analysis of the problem in which to smooth out the stress distribution along the interface, an extrapolation technique based on internal points of the element is used prior to averaging (Wang and Stango, 1983). The approach adopted in this paper was to emphasize that when both possible singularities are included the stress distribution is sufficiently good without extrapolation. When some of the existing singularities are removed, though, this is not necessarily the case. Thus importance of both of the singular terms is additionally demonstrated that way.

Various solutions exist for the (45°/−45°) composite (Pipes and Pagano, 1970; Herakovich *et al.*, 1976; Wang and Crossman, 1977; Wang and Choi, 1982a, b; Wang and Yuan, 1983), this case has been therefore selected here as a kind of benchmark problem. The results presented in Table 1 and on Fig. 3 show that the approach adopted here is equally accurate as far as stress disribution and parameters specifying singularities are concerned. Although the results presented here have been obtained for the discretization shown on Fig. 2, calculations were also made for coarser meshes and the corresponding results were only slightly worse. The errors were within a few percent.

The second problem considered here was the (90°/15°) composite. As can be seen in Zwiers *et al.* (1982), for this orientation a strong log r singularity should exist (see Fig. 5 in Zwiers *et al.* (1982)). Three different groups of results were obtained by including either

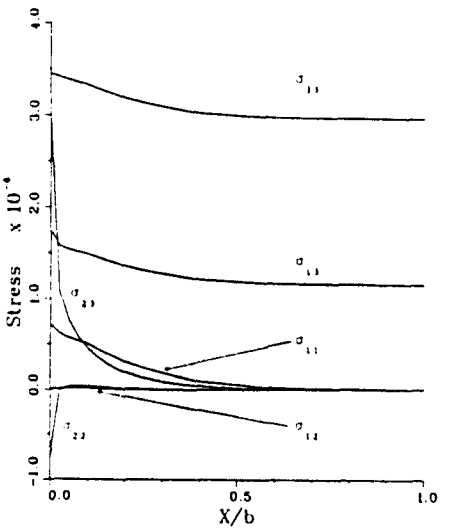

Fig. 3. Stress distributions for (45°/45°) composite laminate.

one or both singular terms with the corresponding unknown coefficients. They are presented in Table 2 and on Figs 4–6. The stresses presented in the figures illustrate their distribution along the interface.

The value $c_1 = 1.038$ in Table 2 seem to be close enough to the theoretical value $c_1 = 1.0$ (see preceding sections) to validate the adopted approach and algorithm. To reach this conclusion one has to take into account the approximate character of the finite element method as well as the complex nature of the interaction between the two singularities in this energy based method. This statement is supported by an increase in c_1 to 1.092 when the r^δ singularity is removed from the model. Similarly, the change of about 10% is recorded in parameters specifying the r^δ singularity when log r terms are removed. From Table 2 and Figs 4–6 we see that the logarithmic singularity has its major effect on the stresses σ_{23}. This influence is so strong that the total value and the logarithmic part of σ_{23} almost coincide as the singular point is approached (Fig. 5(a)). However, Fig. 5(a) also reveals that the interaction of the two singularities is more complex than that. It is seen that while r^δ in σ_{23} approaches ∞ the log r term approaches $-\infty$. Since the r^δ singularity is stronger than log r, in the extremely small neighborhood of the singular point the sign of σ_{23} must be positive despite the impression given by Fig. 5(a). In addition to that the r^δ term has a relatively large influence on the stress components σ_{22} and σ_{12} within the element including the singularity point. This can be deduced by comparing the results obtained without the r^δ term, presented in Figs 4(c) and 6(c), with those in Figs 4(a) and 6(a), respectively, where both singularities are included.

In addition to Zwiers *et al.* (1982), the logarithmic singularity has been also discussed in Davet and Destuynder (1986). The latter paper deals only with a special case in which $\theta_2 = \theta_1 + 90°$ and, in this context, seems to suggest that no other (than logarithmic) singularity exists. On the other hand solution of the eigenvalue problem defined by eqn (A16) gives $\delta_2 = -0.0302747$ which clearly shows that the singularity of the type r^δ, $\delta < 0$ is also possible. To provide some additional insight into this case we consider as the third example the (−15°/75°) composite. The results are included in Table 3 and on Figs 7–9.

There are few interesting aspects of these results. First, contrary to the implication of Davet and Destuynder (1986), the r^δ singularity is present in this problem. The second aspect is that, relative to the log r term, its significance in the overall picture is smaller than in the case of the (90°/15°) composite. This is reflected in a dramatic change of parameters specifying the r^δ singular term when the log r part is excluded from the model. Another interesting observation is that, as in the case of the (90°/15°) composite, the logarithmic terms contribute mainly to σ_{23} (see Davet and Destuynder (1986)) of the three interface stress components. As can be seen by comparing Figs 5(a) and 8(a), however, this time the r^δ and log r contributions to σ_{23} are complementary rather than competing, they both approach $-\infty$. As far as σ_{22} and σ_{23} is concerned, examination of Figs 7(a)–(c) and 9(a)–(c) reveals, that erroneous distribution of those stress components in the elements adjacent to the singular point occurs no matter which of the singularities is excluded from the model; both of them are therefore essential. Finally, the resulting values of c_1 are close enough to the theoretical value $c_1 = 1.00$ to say that the self-imposed check of the model and of the algorithm is passed.

Table 2. Characteristics of singularities for (90°/15°) composite ($\delta = -0.0328141$)

Parameter	r^δ and log r included	Only r^δ included	Only log r included
C_1	1.038	—	1.092
C_2	−31.225	−34.424	—
S^δ_{22}	4.301	4.742	—
S^δ_{23}	0.271	0.299	—
S^δ_{21}	−0.438	−0.438	—
S^l_{22}	0.000	—	0.000
S^l_{23}	0.714	—	0.751
S^l_{21}	0.000	—	0.000

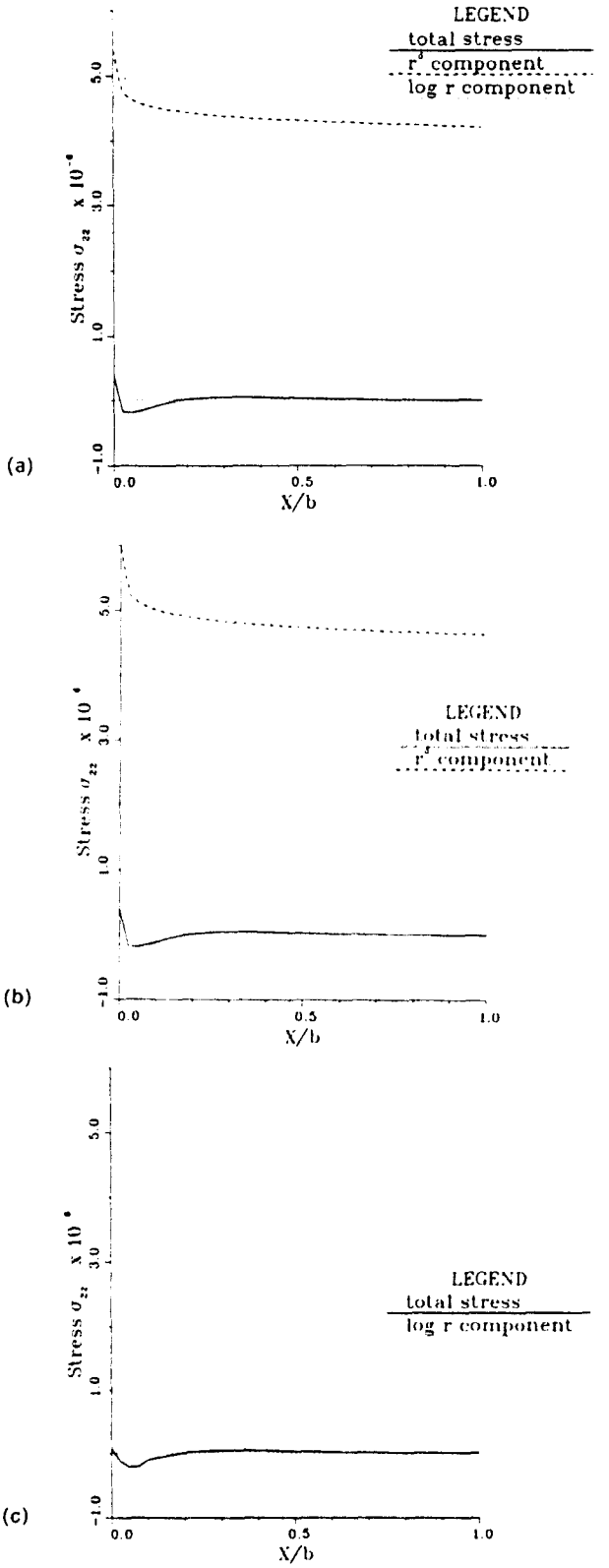

Fig. 4. Interlaminar normal stresses σ_{22} for (90 / 15) composite laminate: (a) r^3 and log r included; (b) r^3 included only; (c) log r included only.

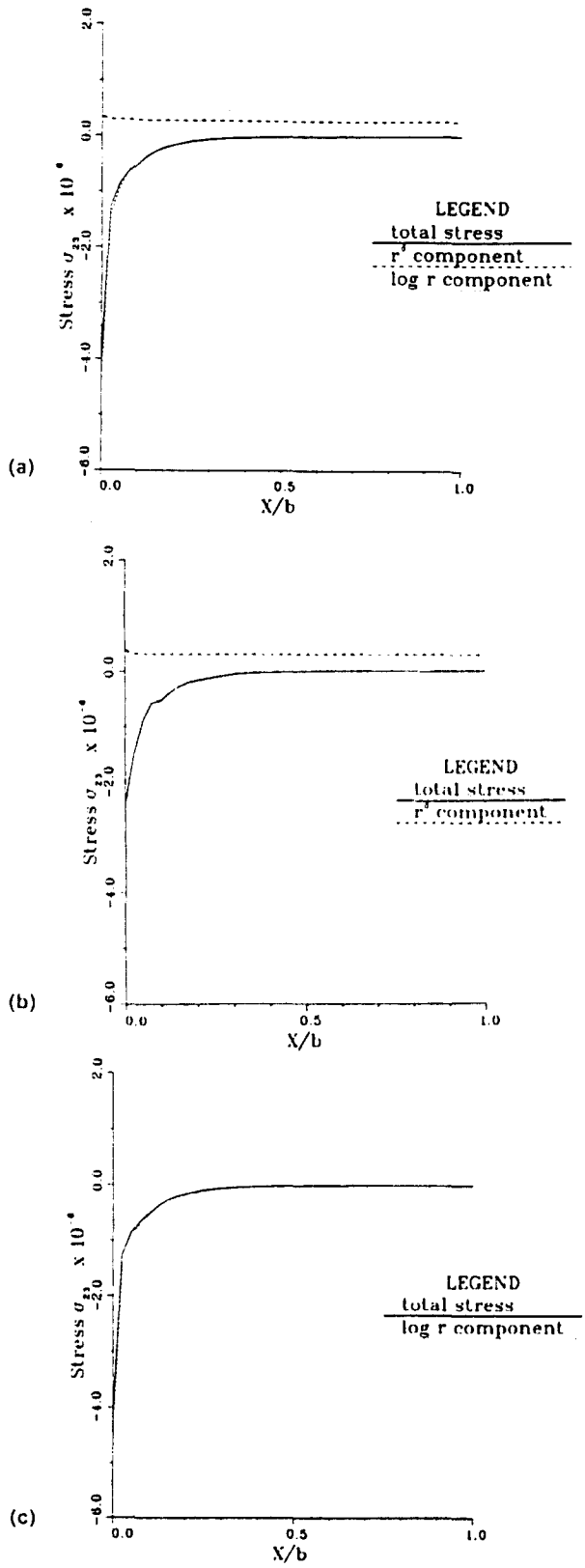

Fig. 5. Interlaminar shear stresses σ_{23} for (90 /15) composite laminate: (a) r^3 and log r included; (b) r^3 included only; (c) log r included only.

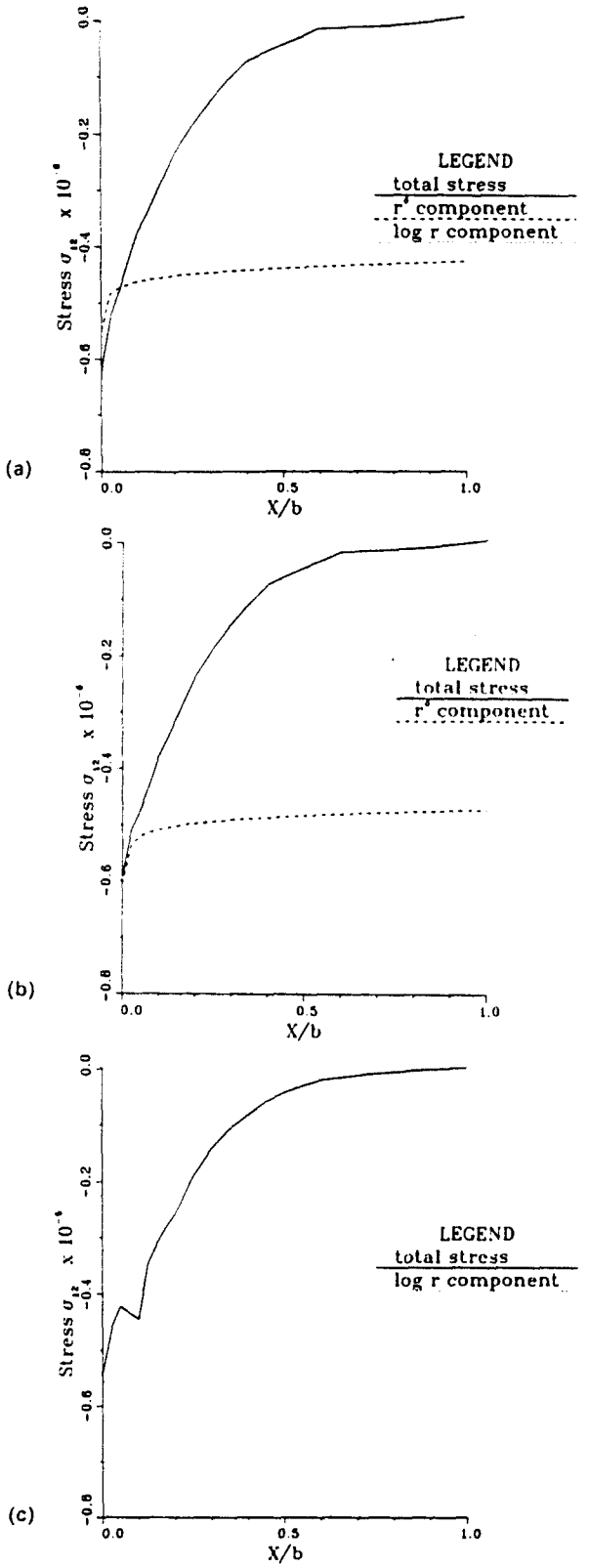

Fig. 6. Interlaminar shear stresses σ_{12} for (90°/15°) composite laminate: (a) r^4 and log r included; (b) r^4 included only; (c) log r included only.

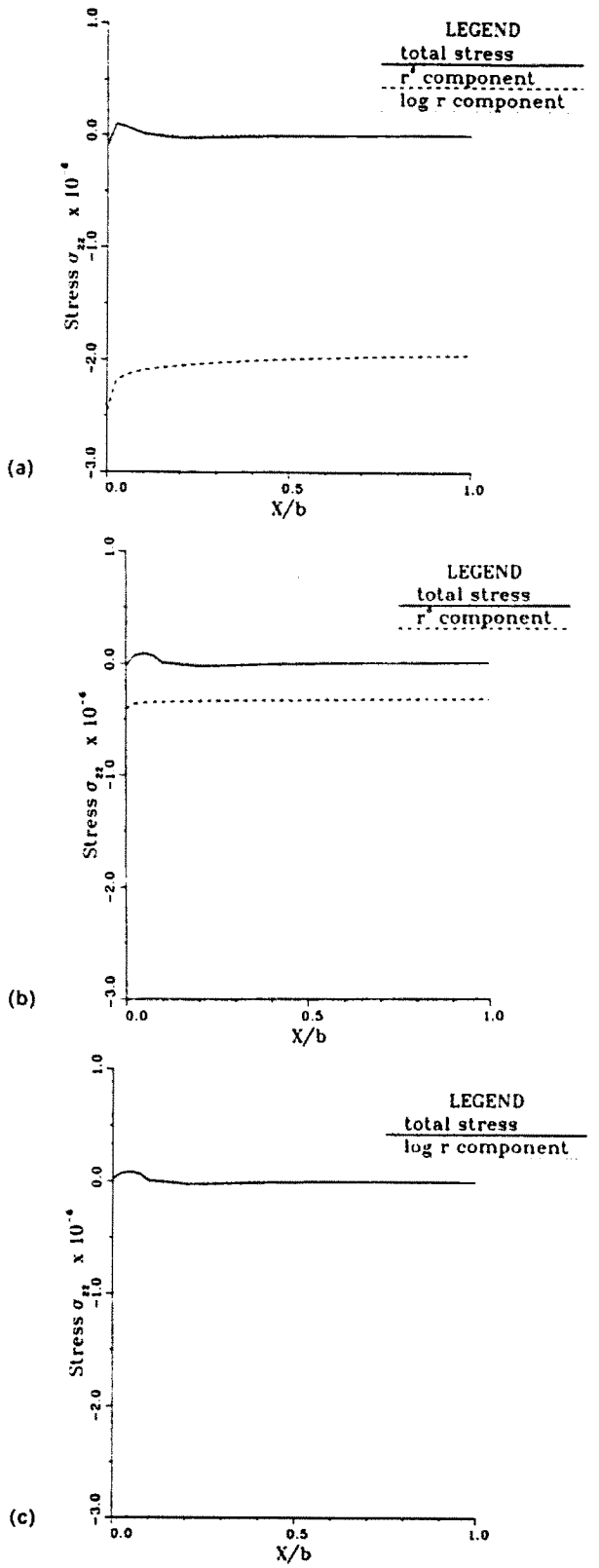

Fig. 7. Interlaminar normal stresses σ_{22} for $(-15^{\circ}/75^{\circ})$ composite laminate: (a) r^3 and log r included; (b) r^3 included only; (c) log r included only.

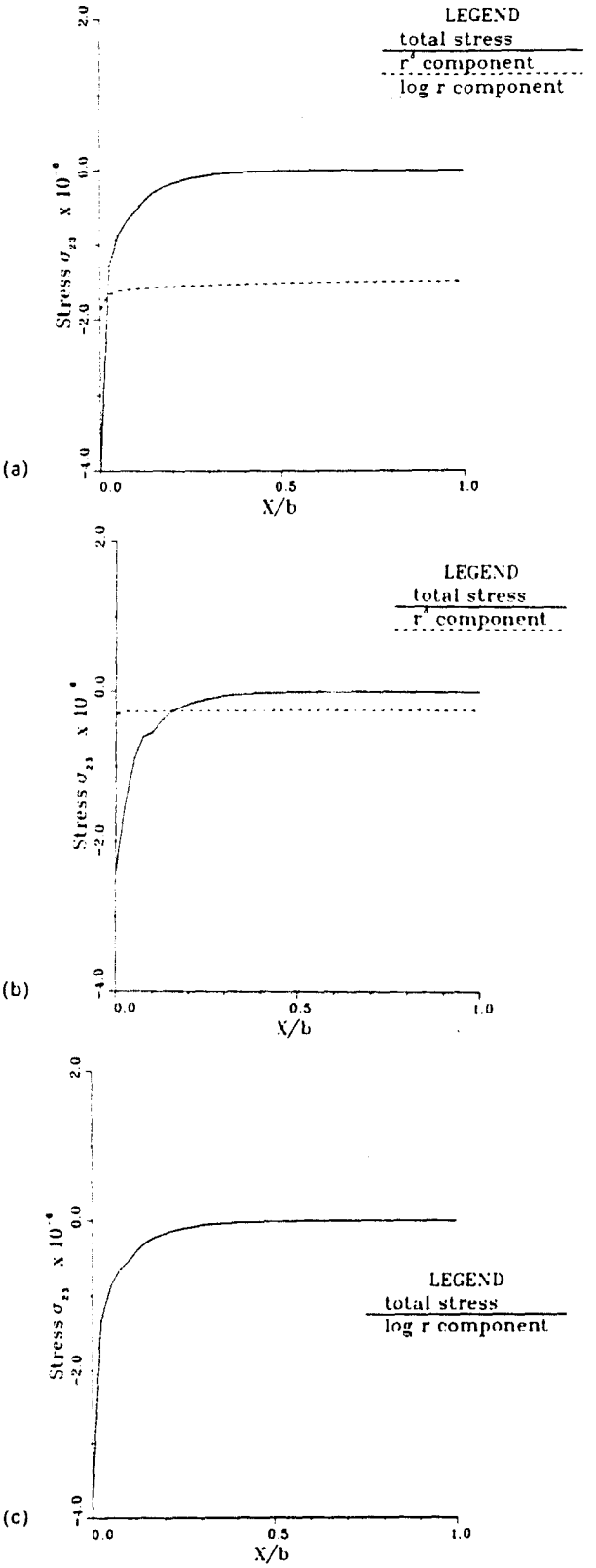

Fig. 8. Interlaminar shear stresses σ_{23} for $(-15^\circ/75^\circ)$ composite laminate: (a) r^3 and log r included, (b) r^3 included only; (c) log r included only.

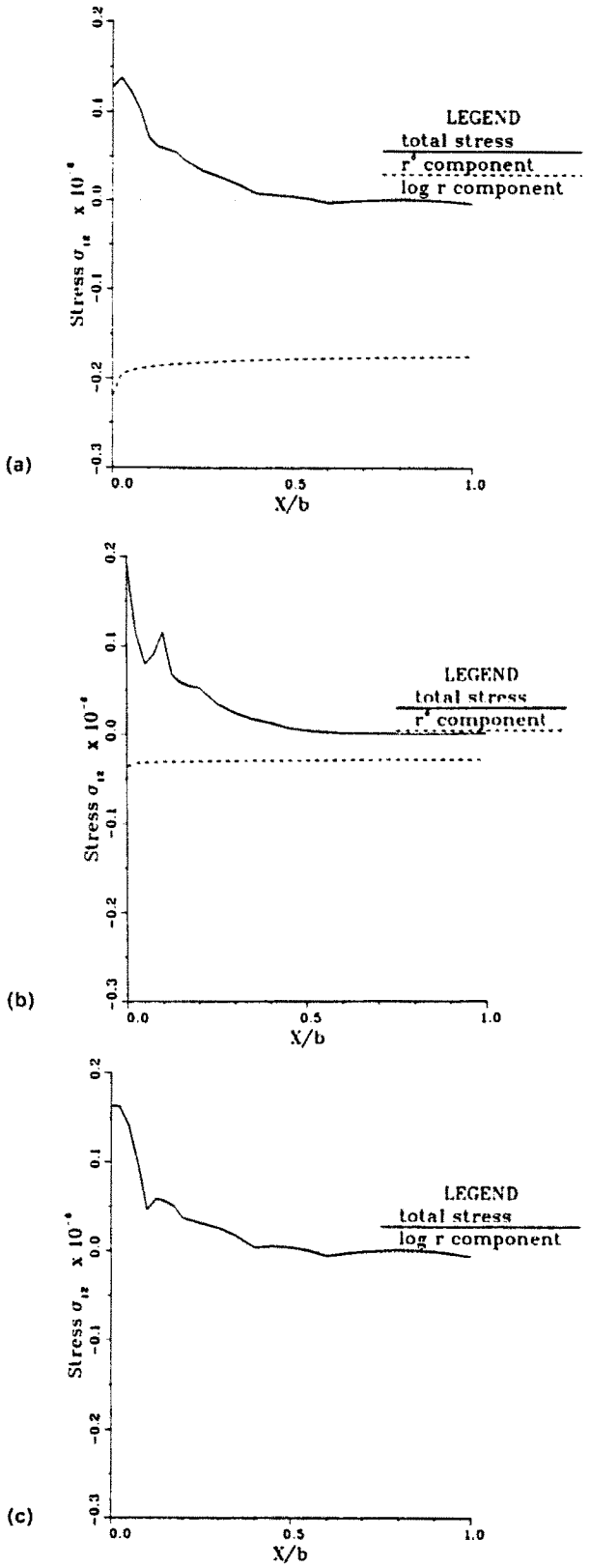

Fig. 9. Interlaminar shear stresses σ_{xz} for $(-15^\circ/75^\circ)$ composite laminate: (a) r^λ and $\log r$ included; (b) r^λ included only; (c) $\log r$ included only.

Table 3. Characteristics of singularities for (−15 75) composite ($\delta = -0.0302747$)

Parameter	r^λ and log r included	Only r^λ included	Only log r included
C_1	1.030	—	0.960
C_2	14.241	2.369	—
S^1_{22}	−1.999	−0.332	—
S^1_{23}	−1.520	−0.253	—
S^1_{21}	−0.179	−0.0297	—
S^l_{22}	0.000	—	0.000
S^l_{23}	0.645	—	0.601
S^l_{21}	0.000	—	0.000

5. CONCLUSIONS

The results presented in this paper clearly show that incomplete theoretical information about the number and/or the type of the singularities involved in a problem may significantly distort the picture emerging from the calculations. Such incompleteness of the information has been modeled here by intentionally retaining in the analysis only one of the two singularities known to be possible in the considered cases. It is shown that in the direct evaluation of stresses along the interface (compare Wang and Stango (1983)) the inaccuracies resulting from an incomplete repesentation of singularities may significantly change the corresponding stress distributions even away from the singular point. Such incompleteness affects also various parameters representing strength of the retained singularity. In some cases, exemplified here by the (−15°/75°) composite analyzed with r^λ as a sole singular term, these parameters can be several times different from those obtained when all of the singularities of the problem are included. These effects are important considering that accurate information about singularities would enable one to assess if a possibility of delamination exists.

The qualitative side of the above results was, to some extent, expected. Quantitatively, however, the numbers obtained show rather dramatically how important it is to combine a careful theoretical analysis of the singularities involved with numerical calculations. For instance, despite the fact that the log r singularity is weaker than the r^λ singularity, and might be expected to play a minor role as far as the results are concerned, its omission in the analysis of the (−15°/90°) laminate changes the strength of the r^λ terms about six times. In this context the discovery of the log r singularity has rather profound significance.

An additional conclusion resulting from the conducted analysis is that, in terms of accuracy and performance, the enriched finite element technique parallels other powerful methods, including the hybrid stress method used for similar calculations in Wang and Choi (1982a, b) and Wang and Yuan (1983).

Acknowledgement—We wish to thank Professor T. C. T. Ting for suggesting the topic for helpful discussions and for providing codes solving the required eigenvalue problems.

REFERENCES

Altus, E., Roten, A. and Shmueli, N. (1980). Free edge effect in angle ply laminates—a new three dimensional finite difference solution. *J. Comp. Mater.* **14**, 21–30.

Atluri, S. N., Kobayashi, A. S. and Nakagaki, N. (1975). An assumed displacement hybrid finite element model for linear fracture mechanics. *Int. J. Fract.* **11**, 257–271.

Bartholomew (1978). Solution of elastic crack problems by superposition of finite elements and singular fields. *Comp. Meth. Appl. Mech. Engng* **13**, 59–78.

Benzley, S. E. (1974). Representation of singularities with isoparametric finite elements. *Int. J. Numer. Meth. Engng* **8**, 537–545.

Byskov, E. (1970). The calculation of the stress intensity factors using the mixed finite element method with cracked elements. *Int. J. Fract. Mech.* **6**, 159–167.

Chen, E. P. (1985). Finite element analysis of a bimaterial interface crack. *Theor. Appl. Fract. Mech.* **3**, 257–262.

Davet, J. L. and Destuynder, Ph. (1986). Free edge stress concentration in composite laminates: a boundary layer approach. *Comput. Meth. Appl. Mech. Engng* **59**, 129–140.

Gallagher, R. H. (1971). Survey and evaluation of the finite element method in fracture mechanics analysis. *Proc. First Int. Conf. SMiRT*, Berlin.
Hartranft, R. J. and Sih, G. C. (1969). The use of eigenfunction expansions in the general solution of three-dimensional crack problems. *J. Math. Mech.* **19**, 123.
Herakovich, C. T. (1976). On thermal edge effects in angle ply composite laminates. *Int. J. Mech. Sci.* **18**, 129–134.
Herakovich, C. T., Renieri, G. D. and Brinson, H. F. (1976). Finite element analysis of mechanical and thermal edge effects in composite laminates. *1976 Army Symp. Solid Mech. Composite Materials, the Influence of the Mechanics of Failure on Design*, Cape Cod, Massachusetts, September, pp. 237–248.
Lin, K. Y. and Mar, J. W. (1976). Finite element analysis of stress intensity factors for cracks at a bimaterial interface. *Int. J. Fract.* **12**, 521–531.
Morley, L. S. D. (1970). A finite element application of the modified Rayleigh–Ritz method. *Int. J. Numer. Meth. Engng.* **2**, 85–98.
Mote, C. D. (1971). Global local finite element. *Int. J. Numer. Meth. Engng* **3**, 565–574.
Pagano, N. J. (1974). On the calculation of interlaminar normal stress in composite laminates. *J. Comp. Mater.* **8**, 65–81.
Pagano, N. J. (1978). Stress fields in composite laminates. *Int. J. Solids Structures* **14**, 385–400.
Pian, T. H. H., Tong, P. and Luk, C. H. (1971). Elastic crack analysis by a finite element hybrid method. *Third Conference on Matrix Methods in Structural Mechanics*, Wright-Patterson Air Force Base, Ohio.
Pipes, R. B. and Pagano, N. J. (1970). Interlaminar stress in composite laminates under-uniform axial extension. *J. Comp. Mater.* **4**, 538–548.
Rybicki, E. F. (1971). Approximate three-dimensional solutions for symmetric laminates under inplane loading. *J. Comp. Mater.* **5**, 354–360.
Spilker, R. L. and Chou, S. C. (1980). Edge effects in symmetric composite laminates. *J. Comp. Mater.* **14**, 2–20.
Tang, S. (1975). A boundary layer theory—Part I: laminate composites in plane stress. *J. Comp. Mater.* **9**, 33–41.
Tang, S. and Levy, A. (1975). A boundary layer theory—II: extensions of laminated finite strip. *J. Comp. Mater.* **9**, 42–45.
Ting, T. C. T. and Chou, S. C. (1981). Edge singularities in anisotropic composites. *Int. J. Solids Structures* **17**, 1057–1068.
Tong, P. and Pian, T. H. H. (1973). On the convergence of the finite element methods for problems with singularity. *Int. J. Solids Structures* **9**, 313–321.
Tong, P., Pian, T. H. H. and Lasry, S. (1973). A hybrid element approach to crack problems in plane elasticity. *Int. J. Numer. Meth. Engng* **7**, 297–308.
Wang, A. S. D. and Crossman, F. W. (1977). Some new results on edge effects in symmetric composite laminates. *J. Comp. Mater.* **11**, 92–106.
Wang, J. T. S. and Dickson, J. N. (1978). Interlaminar stresses in symmetric composite laminates. *J. Comp. Mater.* **12**, 390–402.
Wang, S. S. and Choi, I. (1982a). Boundary layer effects in composite laminates: Part I—free edge stress singularities. *J. Appl. Mech.* **49**, 541–548.
Wang, S. S. and Choi, I. (1982b). Boundary layer effects in composite laminates: Part II—free edge stress solutions and basic characteristics. *J. Appl. Mech.* **49**, 549–560.
Wang, S. S. and Yuan, F. G. (1983). A singular hybrid finite element analysis of boundary-layer stresses in composite laminates. *Int. J. Solids Structures* **19**, 825–837.
Wang, S. S. and Stango, R. J. (1983). Optimally discretized finite elements for boundary-layer stresses in composite laminates. *AIAA J.* **21**, 614–620.
Zwiers, R. I., Ting, T. C. T. and Spilker, R. L. (1982). On the logarithmic singularity of free-edge stress in laminated composites under uniform extension. *J. Appl. Mech.* **49**, 561–569.

APPENDIX

Derivation of the displacement field related to r^{λ} and $\log r$ singularities will be outlined here.

Referring to the coordinate system shown on Fig. 1 and recalling independence of the stress and strains on x^3 (see Section 2) the following equilibrium equations are deduced for the present problem:

$$\sigma_{11,1} + \sigma_{12,2} = 0. \tag{A1}$$

They are combined with the kinematic and constitutive equations

$$\varepsilon_{ij} = \tfrac{1}{2}(u_{i,j} + u_{j,i}) \tag{A2}$$

$$\sigma_{ij} = C_{ijkl}\varepsilon_{kl} \tag{A3}$$

to form the complete set of governing equations.

In the finite element implementation of the problem the components of the strain and stress tensors will form the following vectors:

$$\boldsymbol{\sigma} = \begin{Bmatrix} \sigma_{11} \\ \sigma_{22} \\ \sigma_{23} \\ \sigma_{13} \\ \sigma_{12} \\ \sigma_{33} \end{Bmatrix}, \quad \boldsymbol{\varepsilon} = \begin{Bmatrix} \bar{\boldsymbol{\varepsilon}} \\ \varepsilon_{33} \end{Bmatrix}, \quad \bar{\boldsymbol{\varepsilon}} = \begin{Bmatrix} \varepsilon_{11} \\ \varepsilon_{22} \\ \varepsilon_{23} \\ \varepsilon_{13} \\ \varepsilon_{12} \end{Bmatrix}. \tag{A4}$$

The component ε_{33} in the strain vector $\boldsymbol{\varepsilon}$ has been isolated because of the independence of the unknown displacement field of x^3; we assume $\varepsilon_{33} = 1$ to specify the intensity of the load.

With notation (A4) the following matrix relationship is equivalent to eqn (A3):

$$\boldsymbol{\sigma} = \mathbf{C}\boldsymbol{\varepsilon} \tag{A5}$$

where the 6×6 matrix $\mathbf{C}$ can be related to the components C_{ijkl} of the material tensor of eqn (A3).

Solution to the governing equations is sought in the following form (Zwiers *et al.*, 1982):

$$u_i = \sum_{\alpha} v_i^{\alpha} f^{\alpha}(z) + \delta_{i3}\varepsilon_{33}x^3 \tag{A6a}$$

$$Z = x^1 + px^2 \tag{A6b}$$

where δ_{ij} is Kronecker's delta, p and v_i^{α} are constants to be determined and f is a set of linearly independent functions. Substitution of the assumed displacement field into the governing equations, eqns (A1)–(A3), shows that u_i of eqn (A6a) may be a solution if

$$D_{ik}v_k^{\alpha} = 0 \tag{A7}$$

for every α, where D_{ik} is independent of α

$$D_{ik} = C_{i1k1} + p(C_{i1k2} + C_{i2k1}) + p^2 C_{i2k2}. \tag{A8}$$

Thus, the constant p of eqn (A6b) has to be selected so that

$$\det(D_{ik}) = 0. \tag{A9}$$

For any value p satisfying eqn (A9), the corresponding eigenvector v_k^{α} can be obtained from eqn (A7). This shows that v_k^{α} are the same for all α's, so the superscript α can be omitted. The related solution defined within to an unspecified yet functions $f^{\alpha}(Z)$, can be subsequently obtained from eqn (A6a).

Considering eqns (A8) and (A9) one can see that eqn (A9) is of sixth order with respect to p, there are therefore six solutions for p. However, one can show (Zwiers *et al.*, 1982), that those are formed of three pairs of complex conjugate values $p_L, \bar{p}_L$, $L = 1, 2, 3$ (the overbar indicates the complex conjugate). Consequently, in view of eqn (A8) there are also three pairs of related eigenvectors $v_{kL}, \bar{v}_{kL}$. In any case, for any function f^{α}, the six eigenvalues and corresponding eigenvectors result in six solutions which because of the linearity of the problem, can be linearly combined to yield a general solution.

Since detecting possible singularities is here of particular interest, the following functions f^{α} are assumed:

$$f^{\alpha}(Z) = Z^{1+\delta_{\alpha}}/(1+\delta_{\alpha}). \tag{A10}$$

For this selection, the stresses resulting from eqns (A2) and (A3) have the form

$$\sigma_{ij} = \sum_{\alpha} \tau_{ij} \frac{\mathrm{d}f^{\alpha}}{\mathrm{d}Z} + C_{ij33}\varepsilon_{33} = \sum_{\alpha} \tau_{ij} Z^{\delta_{\alpha}} + C_{ij33}\varepsilon_{33} \tag{A11a}$$

$$\tau_{ij} = (C_{ijk1} + pC_{ijk2})v_k \tag{A11b}$$

which results in a singularity at $x^1 = x^2 = 0$ if, for the same α, $\delta_{\alpha} < 0$. As explained in the previous paragraph combination of the above expressions related to different values of p_L (and $\bar{p}_L$) gives

$$u_i = \sum_{\alpha} \sum_{L=1}^{3} (A_L^{\alpha} v_{iL} Z_L^{1+\delta_{\alpha}} + B_L^{\alpha} \bar{v}_{iL} \bar{Z}_L^{1+\delta_{\alpha}})/(1+\delta_{\alpha}) + \delta_{i3}\varepsilon_{33}x^3 \tag{A12}$$

while the related stress components are expressed as follows:

$$\sigma_{ij} = \sum_{\alpha} \sum_{L=1}^{3} (A_L^{\alpha} \tau_{ijL} Z_L^{\delta_{\alpha}} + B_L^{\alpha} \bar{\tau}_{ijL} \bar{Z}_L^{\delta_{\alpha}}) + C_{ij33}\varepsilon_{33}. \tag{A13}$$

Everything described so far has to be done for each layer of the composite separately (since eqn (A3) is different in each layer) but with the same f^{α}. The resulting two functions, each having the form given in eqns (A12) and (A13), have to be now combined to meet six interface compatibility conditions (three for stresses and three for displacements) and six free edge stress conditions (three for each layer). The resulting 12 equations have the following mathematical structure:

$$\sum_{\alpha} r^{\delta_{\alpha}} \mathbf{M}_{\alpha}(\delta_{\alpha})\mathbf{q}_{\alpha} = \varepsilon_{33}\mathbf{b} \tag{A14}$$

in which $\mathbf{q}^{\alpha}$ combines six constants A_L^{α}, B_L^{α}, $L = 1, 2, 3$ for each layer, $\mathbf{b}$ results from the presence of the term involving ε_{33} in eqns (A12) and (A13), and r is the radius in the polar coordinate system (Fig. 1). The presence of an arbitrary value of r in eqn (A14) indicates that to satisfy eqn (A14), one of the δ_{α}'s say δ_1, must be zero and

$$\mathbf{M}_1(0)\mathbf{q}_1 = \varepsilon_{33}\mathbf{b} \tag{A15}$$

$$\mathbf{M}_{\alpha}(\delta_{\alpha})\mathbf{q}_{\alpha} = \mathbf{0}, \quad \alpha = 2, 3, \ldots \tag{A16}$$

The first of the above equations gives a particular solution, while from the second equation transpires that for the problem to have a singularity the equation

$$\det [\mathbf{M}_c(\delta)] = 0 \tag{A17}$$

must have a solution δ_s the real part of which is $\mathrm{Re}\,\delta_s < 0$. This negative value (or values) of δ_s along with corresponding eigenvectors $\mathbf{q}_s$, obtained from eqn (A16), define the form of the singular contribution to the displacement field given in eqn (A12). In general both δ_s (the one with $\mathrm{Re}\,\delta_s < 0$) and corresponding A_L^s, B_L^s for both layers may be complex. Results reported by Zwiers *et al.* (1982) seems to indicate, however, that there exists only a single real negative root of eqn (A17) which we denote $\delta_2 = \delta$ and which represents the r^δ singularity. In this case, the real solution can be obtained by combining the real and imaginary parts of $v_L Z_L^{1+\delta}$. Thus

$$u_i^2 = \sum_{L=1}^{3} \{A_L\ \mathrm{Re}\,(v_{iL} Z_L^{1+\delta}) + B_L\ \mathrm{Im}\,(v_{iL} Z_L^{1+\delta})\}/(1+\delta) \tag{A18}$$

where A_L and B_L (as well as δ) are now real. All of those numbers can be obtained by solving the eigenvalue problem similar to that given in eqn (A16) which can be readily obtained according to the procedure that has been just described assuming u_i^2 of eqn (A18) for the displacement field (Zwiers *et al.*, 1982). As in any eigenvector problem the eigenvector $\mathbf{q}_2$ is defined within a multiplicative constant and, thus, so is the displacment field u_i^2.

The logarithmic singularity comes about because of the difficulties with the satisfaction of Eqn (A15). It appears that the matrix $\mathbf{M}_c(0)$ is always singular and a solution of eqn (A15) exists only when the vector $\mathbf{b}$ belongs to the space spanned by linearly independent columns of $\mathbf{M}_c(0)$. Such a special situation happens to occur only under special circumstances, namely for $(\theta/-\theta)$ laminates and a particular family (θ_1/θ_2) composites (Zwiers *et al.*, 1982). In general eqn (A15) cannot be satisfied.

The above situation indicates that, in general, for $\delta_1 = 0$ the solution cannot have the form given in eqn (A10) and in the corresponding eqn (A12). To rectify the problem, a different solution for $\delta_1 = 0$ has been obtained in Zwiers *et al.* (1982) by means of the following technique:

$$u_i^1 = \frac{\partial f}{\partial \delta_1} \left\{ \sum_{L=1}^{3} [A_L\ \mathrm{Re}\,(v_{iL} Z_L^{1+\delta_1}) + B_L\ \mathrm{Im}\,(v_{iL} Z_L^{1+\delta_1})]/(1+\delta_1) \right\}_{\delta_1 = 0} + \varepsilon_{11} \delta_{i1} x^1. \tag{A19}$$

Differentiation present in the above equation is performed assuming that A_L and B_L depend on δ_1 and leads to the following result:

$$u_i^1 = \sum_{L=1}^{3} [A_L\ \mathrm{Re}\,(v_{iL} Z_L \log Z_L) + B_L\ \mathrm{Im}\,(v_{iL} Z_L \log Z_L)] + \sum_{L=1}^{3} [A_L^1\ \mathrm{Re}\,(v_{iL} Z_L) + B_L^1\ \mathrm{Im}\,(v_{iL} Z_L)] + \varepsilon_{11} \delta_{i1} x^1 \tag{A20}$$

where A_L^1, B_L^1, $L = 1, 2, 3$ is a set of new constants. Thus the solution given by eqn (A20) is, in each layer, defined in terms of 12 constants A_L, B_L, A_L^1, B_L^1, $L = 1, 2, 3$. They have to be determined from the same interface and boundary conditions which previously led to eqn (A15). This time, the resulting system of equations has the following form:

$$\mathbf{M}(0)\mathbf{q}_1 = \mathbf{0} \tag{A21a}$$

$$\mathbf{M}^1(0)\mathbf{q}_1 + \mathbf{M}(0)\mathbf{q}_1^1 = \varepsilon_{11}\mathbf{b} \tag{A21b}$$

where $\mathbf{M}(0)$ and $\mathbf{q}_1$ is the same as in eqn (A15) while $\mathbf{M}^1(0)$ is a new 12×12 matrix and $\mathbf{q}_1^1$ contains constants A_L^1 and B_L^1.

In view of eqn (A20) it is clear that only the vector $\mathbf{q}_1$ of eqns (A21a) and (A21b) is related to the logarithmic term $\log Z_L$. The underlined part of eqn (A20) is linear, therefore it can be well represented by the regular finite element shape functions and omitted in the singular logarithmic displacement field. As shown in Zwiers *et al.* (1982) the vector $\mathbf{q}_1$ that defines this singular field is uniquely determined from eqns (A21), and so is the field itself. If $\mathbf{q}_1 = 0$ no logarithmic singularity exists.